Theor Chim Acta (1991) 79: 93–103

Theoretica
Chimica Acta

Computation of electronic transition moments: the length versus the velocity representation

Charles W. Bauschlicher, Jr. and Stephen R. Langhoff
NASA Ames Research Center, Moffett Field, CA 94035, USA

Received August 6, 1990; received in revised form September 24, 1990/Accepted September 26, 1990

Summary. We have compared transition moments (TMs) obtained using the length and velocity representations for transitions from the ground state of H_2 to the lowest two $^1\Pi_u$ and two $^1\Sigma_u^+$ Rydberg states, the $A^1\Pi$–$X^1\Sigma^+$ transition in BH, and the $A^1\Pi_u$–$X^1\Sigma_g^+$ transition in C_2. For H_2, the TMs in the length and velocity representations agree well even in cases where the one-particle basis is incomplete and the TM has not converged. For BH and C_2 the TM in the length representation converges rapidly with improvements in the one-particle basis set and is insensitive to inner-shell correlation. In contrast, in the velocity representation convergence with improvements in the one-particle basis is much slower, especially for C_2, and the TMs are significantly changed by inner-shell correlation. Thus the difference between the TMs in the length and velocity representations would not appear to be a viable diagnostic of TM convergence.

Key words: Transition moments – Convergence – Length representation – Velocity representation

1. Introduction

Ab initio calculations have been very useful in defining the form of transition moments (TMs) as a function of geometry. It is often very difficult to deduce this information from experiment because of the very limited geometry variation sampled in either emission or absorption. More recently *ab initio* calculations have begun to reach such a level of accuracy that they can not only determine the functional form, but also reliably determine lifetimes and Einstein coefficients [1]. One problem with the *ab initio* approach is that it is often difficult to assess the accuracy of the computed moment, which ultimately depends on the truncation of the one- and n-particle basis sets used in the approximate solution of the Schrödinger equation. Full configuration-interaction (FCI) benchmark calculations have given new insight into the correlation problem, and the development of new basis sets has reduced the error associated with the one-particle expansion [1]. With these advances it is now possible to systematically expand both the one- and n-particle spaces such that a measure of the convergence of the results is obtained, but an easily calculated quantity that gives a measure of the reliability would still be invaluable. This is especially true where demonstrating convergence in both the one- and n-particle spaces is currently not feasible. One possible measure of this convergence could be the difference between the TM computed using different representations of the dipole operator.

The transition moment for an n-electron system can be computed using one of the length, velocity or acceleration representations, which are given as [2]

$$\langle \Psi_a | \sum_{k=1}^{n} r_k | \Psi_b \rangle, \tag{1}$$

$$(E_a - E_b)^{-1} \langle \Psi_a | -i \sum_{k=1}^{n} \nabla_k | \Psi_b \rangle, \tag{2}$$

and

$$(E_a - E_b)^{-3} \langle \Psi_a | - \sum_{k=1}^{n} \nabla_k V | \Psi_b \rangle, \tag{3}$$

respectively, where Ψ_a and E_a are the wave function and energy of state a and V is the potential energy. The TM computed in these three representations will agree for the exact wave function, i.e. a complete configuration-interaction (CI) wave function (FCI in an infinite (complete) one-particle basis). Previous work has shown [3] that the convergence of the TM generally follows the sequence length faster than velocity, which in turn is much faster than acceleration. Closure tests have shown [4] that for modest sized basis sets the length representation is expected to be much more accurate than the velocity representation. It is therefore not surprising that in virtually all bound-state calculations the TM is computed using the length representation. The TM in the velocity representation is sometimes determined as a qualitative check on the length representation, but it has not been shown how the difference in the TM with representation is related to the error in the length value. Given the recent advances in techniques for systematically improving *ab initio* calculations, it is timely to reinvestigate the convergence of TMs in the velocity and length representations.

In this work we study the convergence of the electronic transition moment in both the length and velocity representations for four Rydberg transitions in H_2, the $A\,^1\Pi - X\,^1\Sigma^+$ transition in BH and the $A\,^1\Pi_u - X\,^1\Sigma_g^+$ (Phillips) band system of C_2. Since the convergence of the acceleration representation is very poor, we do not consider it here. FCI calculations are used to calibrate the n-particle space, while basis set extension is used to explore convergence in the one-particle space. We also consider correlation of the core orbitals, as the velocity results depend more heavily on the description of the inner portions of the wave function. Although the velocity form of the dipole operator has proven useful in determining photoionization cross sections [5], our results demonstrate that for bound-bound transitions in molecular systems studied with conventional n-particle treatments such as CI, the transition moment converges far more quickly in the length representation. In fact, the convergence of the TM in the velocity representation with improvements in wave function quality can be sufficiently slow to preclude its use as a meaningful diagnostic of the convergence of the length TM.

2. Computational methods

Gaussian basis sets are used exclusively in this work. The atomic natural orbital (ANO) procedure [6] is used to contract large primitive sets, which are then supplemented by adding diffuse functions or by uncontracting the outermost primitive functions in the ANO basis set. A ratio of 2.5 is used between exponents in both the added polarization functions and diffuse functions. Only the pure spherical harmonic components of the basis functions are used. Further details of the basis sets are given in the subsequent discussion of the individual molecules.

The orbitals are optimized using the state-averaged complete-active-space self-consistent-field (SA-CASSCF) approach. While the calculations are performed in C_{2v} or D_{2h} symmetry, full $C_{\infty v}$ or $D_{\infty h}$ symmetry is imposed on the orbitals [7]. More extensive correlation is added using the MRCI approach. In some calculations we include all configurations in the CASSCF as references (denoted CAS-Ref). However, when this led to prohibitively large CI expansions, we selected references based on their importance in the CASSCF wave function. The reference lists included all occupations for which the absolute value of the coefficient of any one of its component spin couplings exceeded a designated threshold in the CASSCF wave function. In general, the transition moment computed in the velocity representation arises from many more contributions, some of which have similar magnitude, but opposite sign. Therefore, the MRCI wave function must be determined to much higher precision to achieve the same accuracy in the velocity TM as in the length TM. In this work we converge the energy to at least $1 \times 10^{-7}\ E_h$, and in most cases $1 \times 10^{-8}\ E_h$. The velocity TM is precise to about 0.003 au, which is sufficient for comparison with the value in the length representation.

The calculations were carried out using the MOLECULE-SWEDEN [8] program system at the NASA Ames Research Center Central Computing Facility.

3. Results and discussion

3.1. H_2

We first consider the transition moments from the ground $^1\Sigma_g^+$ state of H_2 at its equilibrium geometry of 1.4 a_0 to the two lowest $^1\Sigma_u^+$ and $^1\Pi_u$ states. These four Rydberg states have been assigned as follows [9]: $(1)\,^1\Sigma_u^+(2p\sigma)$, $(1)\,^1\Pi_u(2p\pi)$, $(2)\,^1\Sigma_u^+(3p\sigma)$, and $(2)\,^1\Pi_u(3p\pi)$. We use ground-state orbitals, but since our treatment corresponds to a FCI treatment, the TMs are invariant to the particular choice of the molecular orbitals.

We should note that these transitions have been studied previously by Rothenberg and Davidson [10]. In their work, the one-particle basis set was fixed and the number of configurations was systematically expanded based on their importance in the CI wave function in terms of natural orbitals. Since they found the length and velocity TMs to have essentially the same sensitivity to the CI expansion, there was no indication that the n-particle requirements were significantly different for the two representations for these transitions in H_2. Thus in our work we focus on the convergence of the one-particle basis set.

The transition energies and the TMs in the length and velocity representations are summarized in Table 1 for a variety of one-particle basis sets,

Table 1. Summary of H_2 results at $1.4\,a_0$. The transition moment, given in both the velocity and length representations, is in au and the vertical energy separation, ΔE, is in cm^{-1}

	Root 1			Root 2		
	ΔE	length	velocity	ΔE	length	velocity
A. [4*s* 2*p* 1*d*] ANO set						
$^1\Sigma_u^+$	116874.6	1.2718	1.2325	239018.3	0.3539	0.3856
$^1\Pi_u$	180758.1	1.1447	0.9915	348453.2	0.0723	0.0895
B. [5*s* 3*p* 1*d*]—set A plus diffuse *s* and *p* functions						
$^1\Sigma_u^+$	103092.7	0.9836	0.9750	124241.6	0.5974	0.5792
$^1\Pi_u$	107611.8	0.7256	0.7143	200930.6	0.9135	0.8184
C. [5*s* 4*p* 2*d*]—set B plus an additional *p* and *d* ANO						
$^1\Sigma_u^+$	103058.2	0.9833	0.9807	124249.5	0.5843	0.5787
$^1\Pi_u$	107390.9	0.7539	0.7493	179409.0	0.8860	0.8388
D. [6*s* 5*p* 2*d*]—set C plus second set of diffuse *s* and *p* functions						
$^1\Sigma_u^+$	102877.9	0.9787	0.9768	119798.0	0.4104	0.4110
$^1\Pi_u$	107026.1	0.7029	0.6948	123149.3	0.4691	0.4679
E. [7*s* 6*p* 2*d*]—set D with outermost *s* and *p* functions uncontracted						
$^1\Sigma_u^+$	102768.9	0.9816	0.9809	119778.6	0.4103	0.4110
$^1\Pi_u$	106624.1	0.7394	0.7378	123096.2	0.4788	0.4776
F. [7*s* 6*p* 3*d*]—set E with outermost *d* function uncontracted						
$^1\Sigma_u^+$	102769.9	0.9816	0.9812	119785.2	0.4108	0.4110
$^1\Pi_u$	106571.6	0.7416	0.7407	123073.1	0.4779	0.4771
G. [7*s* 6*p* 4*d* 2*f*]—set D with a third set of diffuse *s* and *p* functions added, the outermost *d* uncontracted, and a diffuse *d* and a (3*f*)/[2*f*] ANO polarization set added						
$^1\Sigma_u^+$	102841.7	0.9802	0.9796	119719.7	0.3973	0.3971
$^1\Pi_u$	106787.0	0.7212	0.7170	120921.7	0.3324	0.3302

designated A through G. We begin with the (8*s* 6*p* 4*d*)/[4*s* 2*p* 1*d*] ANO set contracted [6] for the $^1\Sigma_g^+$ ground state of H_2. As this basis set lacks diffuse functions, the excited states are poorly described: the vertical excitation energies are up to 200 000 cm^{-1} larger than the experimental T_e values [9]. Nevertheless, the length and velocity TMs agree reasonably well. Adding even-tempered diffuse *s* and *p* functions (scale factor of 2.5) dramatically improves the energy separations. The TMs in the velocity and length representations now agree well for transitions to the lowest three Rydberg states. Adding a second *d* ANO has little effect except to reduce the (2) $^1\Pi_u$ state vertical excitation energy by about 20 000 cm^{-1} and to improve the agreement between the velocity and length TMs for the (2) $^1\Pi_u$–$X^1\Sigma_g^+$ transition. However the (2) $^1\Pi_u$ state is still very poorly described in this basis set. Adding a second set of even-tempered diffuse *s* and *p* functions lowers the excitation energies further, especially for the (2) $^1\Pi_u$ state. In this basis set the velocity and length TMs agree very well for all four transitions studied. Uncontracting the outermost *s*, *p*, and *d* primitive functions to give set F has essentially no effect on the results. An analysis of the (2) $^1\Pi_u$ state natural orbitals shows that the most diffuse *p* function in the strongly occupied π orbital has the largest weight; this suggests that this state is not converged with respect to basis set. On the other hand, the very small difference between the TMs in the velocity and length representation could be interpreted as indicating convergence. To test convergence, a third set of diffuse s and p functions, a diffuse d function, and a $(3f)/[2f]$ ANO polarization set were added to give set G. This large increase in basis set size reduces all of the TMs, but only the $(2)\,^1\Pi_u$–$X^1\Sigma_g^+$ transition changes significantly.

Inspection of Table 1 shows that the difference between the TMs in the length and velocity representations is often much smaller than the error in the TMs due to basis set incompleteness. This is well exemplified by comparing the results for the $(2)\,^1\Pi_u$–$X^1\Sigma_g^+$ TMs in basis sets F and G—see Table 1. This TM is reduced by 0.1455 au (in the length representation) when the F basis is augmented to give set G, whereas the velocity and length TMs differ by only 0.008 au in basis set F. Thus the difference between the TMs in the velocity and length representations in this case suggest incorrectly that the TM in basis set F is accurate.

3.2. BH $A^1\Pi$–$X^1\Sigma^+$ *transition*

The $A^1\Pi$ state of BH lies 23 136 cm^{-1} above the $X^1\Sigma^+$ state [9]. This excited state is dominantly valence in character, although it does contain some contribution from the more diffuse $^2D(2s^12p^2 + 2s^23d^1)$ atomic state. Thus this valence-valence transition could potentially show very different convergence behavior of the TMs in the velocity and length representations than do the H_2 valence-Rydberg transitions.

The boron primitive basis set consisted of the $(13s\ 8p)$ set of van Duijneveldt [11] supplemented with a $(6d\ 4f\ 2g)$ even-tempered polarization set. The hydrogen basis set was the $(8s\ 6p\ 4d)$ primitive set used previously for H_2. We studied the A–X TMs at $r = 2.35\,a_0$ near the equilibrium geometry of both states. Electron correlation was included using the CAS-Ref MRCI procedure.

The vertical excitation energy and the TMs in the length and velocity representations are summarized for the A–X transition of BH in Table 2. We first consider the convergence of the n-particle treatment using a $[4s\ 3p\ 2d\ 1f]/[4s\ 2p\ 1d]$ ANO basis set. The smallest CASSCF active space employed includes the B $2s$ and $2p$ and H $1s$ orbitals and electrons. Since this corresponds to three a_1, one b_1 and one b_2 orbital in C_{2v} symmetry, it is denoted as CASSCF(*3110*). The FCI is performed using these orbitals correlating four electrons, i.e. the boron $1s$-like electrons are not correlated. The transition moments in the velocity and length representation differ by 14% at the FCI level. The CASSCF(*3110*)/MRCI treatment agrees well with the FCI for the energy separation and length TM, but differs slightly with the velocity TM. Expanding the active space to (*5220*) substantially improves the agreement with the FCI. Deleting the σ active orbital with the smallest occupation number and adding a third π and δ orbital to the active space to give a CASSCF(*5331*)/MRCI treatment further improves the results slightly, while restoring the sixth σ orbital to the active space has little additional effect. We note that it was also necessary [12] to expand the active space beyond (*3110*) to obtain an accurate D_e, T_e, and barrier in the $A\,^1\Pi_u$ state. While the (*5220*) and (*5331*) active spaces yield comparable TMs, we use the (*5331*) active space for the one-particle calibration, as this larger active space is necessary to describe the full $A\,^1\Pi$ state potential accurately.

Our initial FCI calculations did not address the importance of boron $1s$ correlation. However, by truncating the ANO basis set to $[4s\ 3p\ 1d/4s\ 1p]$, we

Table 2. Summary of the $A^1\Pi - X^1\Sigma^+$ transition in BH at $r = 2.35\,a_0$. The transition moment is given in au and the vertical energy separation, ΔE, is in cm^{-1}

	ΔE	length	velocity
Calibration of *n*-particle treatment in [4*s* 3*p* 2*d* 1*f*/4*s* 2*p* 1*d*] ANO basis set			
FCI	23505	0.5708	0.6487
CASSCF(*3110*)/MRCI	23538	0.5700	0.6304
CASSCF(*5220*)/MRCI	23541	0.5703	0.6465
CASSCF(*5331*)/MRCI	23511	0.5707	0.6505
CASSCF(*6331*)/MRCI	23512	0.5708	0.6511
Effect of 1*s* correlation in [4*s* 3*p* 1*d*/4*s* 1*p*] basis set			
FCI	24113	0.5864	0.6789
FCI(1*s*)	24050	0.5869	0.6461
Calibration of one-particle basis set using the CASSCF(*5331*)/MRCI treatment			
A. [4*s* 3*p* 2*d* 1*f*/4*s* 2*p* 1*d*]	23511	0.5707	0.6505
B. + 1*s* corr	23427	0.5711	0.6173
C. + B *f* uncont	23461	0.5706	0.6485
D. + B *d* and *f* uncont	23417	0.5599	0.6054
E. + B *d* and *f* uncont + 1*s* corr	23310	0.5599	0.5729
F. + B *d* and *f* uncont + B diffuse *f*	23417	0.5599	0.6054
G. + B *d* and *f* uncont + B tight *f*	23417	0.5600	0.6054
H. minus B *f* ANO	23878	0.5665	0.6210
I. minus B *f* and H *d* ANO	23873	0.5675	0.6336
J. minus B *f* and H *d* ANO + B *d* uncont	23838	0.5571	0.5900
K. minus B *f* and H *d* ANO + B *d* uncont + 1*s* corr	23742	0.5569	0.5577
L. minus B *f* and H *d* ANO + B *p* and *d* uncont	23776	0.5633	0.6032
M. minus B *f* and H *d* ANO + B *s*, *p* and *d* uncont	23773	0.5649	0.6031
N. minus B *f* and H *d* ANO + B *p* and *d* and H *p* uncont	23758	0.5592	0.5999
O. minus B *f* and H *d* ANO + B *d* uncont + two tight B *d*	23838	0.5571	0.5900
P. [5*s* 6*p* 5*d* 2*f* 1*g*/4*s* 3*p* 2*d*]	23319	0.5674	0.6190
Q. [7*s* 9*p* 7*d*/4*s* 2*p*]	23772	0.5651	0.6031
R. [7*s* 9*p* 7*d*/4*s* 2*p*] + 1*s* corr	23658	0.5606	0.5647

were able to perform six-electron FCI calculations. We find that the energy separation and length TM are hardly changed by 1*s* correlation, but that the velocity TM is reduced by about 5%, bringing it into somewhat better agreement with the length representation—see Table 2. Thus the velocity TM is much more sensitive to core correlation than the length TM.

The results of the one-particle basis set calibration using the CASSCF(*5331*)/MRCI treatment are also given in Table 2. The first entry is the [4*s* 3*p* 2*d* 1*f*/4*s* 2*p* 1*d*] basis set used in the *n*-particle calibration study. Adding boron 1*s* correlation reduces the velocity TM by a comparable amount as found at the FCI level. The velocity TM is found to be considerably more sensitive to changes in the one-particle basis than the length TM. One of the largest changes in the TMs occurs upon uncontracting the B *d* basis; this reduces the velocity TM by about four times as much as the length, bringing the values in the two representations into better agreement. However, uncontracting the B *s* and *p* or the H *p* functions had little effect on the TM in either representation. Furthermore, both moments are relatively insensitive to uncontracting the boron *f* set or adding either a diffuse or tight *f* function to boron. Also, the effect of 1*s* correlation is found to be insensitive to changes in the valence basis.

The largest basis set employed for boron was the set used [12] to compute the BH dissociation energy and the barrier in the $A^1\Pi$ state. This basis set was derived from the [5*s* 4*p* 3*d* 2*f* 1*g*] ANO set. The outermost *p* and *d* primitives were uncontracted and a diffuse even-tempered *p* and *d* function were added. In this very large set, the velocity and length TMs still differ by 0.0516 au. The calculations in the smaller basis sets suggest that 0.032 au of this difference is due to neglect of 1*s* correlation, which in this basis increases the size of the CI expansion from only 130 000 to more than 2.4 million configuration state functions.

Since the previous calculations may have underestimated the effect of 1*s* correlation due to basis set limitations, we performed an additional calculation in a basis set flexibly contracted in the core region. Specifically, the seven inner *s* functions were contracted using the SCF 1*s* orbital, but the remaining *s* functions were uncontracted. The inner two *p* functions were replaced by three even-tempered functions and all nine *p* functions were uncontracted. An even-tempered tight *d* function was added and all seven *d* functions were uncontracted. The [4*s* 2*p*] hydrogen basis set was used. This basis set recovers almost five times as much core correlation as our other basis sets. In this basis set we find a small 0.8% reduction in the length TM due to core correlation. Core correlation reduces the velocity TM by 0.038 au, compared with 0.032 au in the smaller sets. This suggests that while most of the difference between the length and velocity representations in our largest basis set (P) arises from core correlation, some probably still arises from the one- and *n*-particle valence treatment.

The observation that the transition moment in the velocity representation is much more sensitive to core correlation is very significant, since in the limit of a complete CI for valence correlation the TM in the length representation will be more accurate than the value in the velocity representation. Correlating the core electrons leads to much longer CI expansions, especially considering that the one-particle basis set requirements are much greater. In fact, in many cases the addition of core correlation makes the calculation computationally intractable. Thus, it seems unlikely that the velocity TM can even be used as a reliable measure of the convergence of the length TM.

3.3. C_2 $A^1\Pi_u$–$X^1\Sigma_g^+$ *Phillips system*

The $X^1\Sigma_g^+$ state of C_2 undergoes an avoided crossing at an r value slightly longer than the r_e for the ground state. Previous work [13] suggested that it was therefore important to include not only the $A^1\Pi_u$ and $X^1\Sigma_g^+$ states in the SA-CASSCF treatment, but also the $(2)\,^1\Sigma_g^+$ state. A series of calculations, calibrated against a FCI treatment, showed [14] that the 3-root SA-CASSCF $A^1\Pi_u$–$X^1\Sigma_g^+$ TM converged more rapidly with reference selection threshold, but that for small thresholds ($\leqslant 0.025$) the 2-root SA-CASSCF TM was also accurate. In this work we study the Phillips band system of C_2 at 2.6 a_0, and consider both the 2-root and 3-root optimizations. The initial ANO basis sets are derived from the (13*s* 8*p* 6*d* 4*f* 2*g*) primitive set described previously [14].

We begin our study using the [3*s* 2*p* 1*d*] ANO basis set averaging for two roots. With a CAS-Ref treatment of electron correlation, the TMs in the velocity and length representations differ by more than 25%—see Table 3. Including 1*s* correlation reduces the velocity TM and leaves the length TM essentially unchanged, thereby increasing the discrepancy between the length and velocity

Table 3. Summary of $A^1\Pi_u$–$X^1\Sigma_g^+$ C_2 transition. The transition moment is given in au and the vertical energy separation, ΔE, is in cm^{-1}

	ΔE	length	velocity
2-root calculations			
[3*s* 2*p* 1*d*] CAS-Ref	6003	0.2768	0.2018
[3*s* 2*p* 1*d*] CAS-Ref(1*s*)	6031	0.2766	0.1668
[3*s* 2*p* 1*d*] MRCI(0.05)	5820	0.3040	0.1077
[3*s* 2*p* 1*d*] MRCI(0.025)	6048	0.2833	0.2041
[4*s* 3*p* 2*d*] MRCI(0.025)	5433	0.2966	0.0246
[4*s* 3*p*(2 + 1)[a]*d*] MRCI(0.025)	5437	0.2940	0.0091
[4*s* 3*p*(2 + 1)*d*] MRCI(0.025)[b]	5427	0.2870	0.0204
[(5 + 1)*s*(4 + 1)*p* 2*d*] MRCI(0.025)	5368	0.3007	0.0677
3-root calculations[c]			
[3*s* 2*p* 1*d*] CAS-Ref	5974	0.2777	0.1398
[3*s* 2*p* 1*d*] CAS-Ref(1*s*)	6006	0.2777	0.0996
[3*s* 2*p* 1*d*] MRCI(0.025)	5997	0.2798	0.1099
[4*s* 3*p*(2 + 1)*d*] MRCI(0.025)	5366	0.2974	0.1281
[(4 + 1)*s*(3 + 1)*p*(2 + 1)*d*] MRCI(0.025)	5290	0.3013	0.2158
[(4 + 1)*s*(3 + 1)*p*(2 + 1)*d*] MRCI(0.025)(1*s*)	5375	0.3019	0.2725
[(4 + 1)*s*(3 + 1)*p*(2 + 1)*d* 1*f*] MRCI(0.025)	5328	0.2999	0.1929
[(4 + 1)*s*(3 + 1)*p* 2*d*] MRCI(0.025)	5303	0.3005	0.1819
[(4 + 1)*s*(3 + 1)*p*(2 + 1)*d*] + (*sp*)[d] MRCI(0.025)	5282	0.3016	0.2218
[(5 + 1)*s*(4 + 1)*p* 3*d* 2*f* 1g] + (*sp*) MRCI(0.025)	5237	0.2924	0.2530
[(5 + 1)*s*(4 + 1)*p*(3 + 1)*d* 2*f* 1g] + (*sp*) MRCI(0.025)	5236	0.2912	0.2552

[a] Indicates two ANOs with the outermost primitive uncontracted

[b] Three-root reference list

[c] MRCI(0.025) calculations use the 0.025 reference list selected based on r values between 1.8 and 5.0 a_0 from ref. [14]

[d] Indicates that an even-tempered s and p function have been added

TMs. We next considered the effect of reference selection on the TMs, since it was not possible to carry out a CAS-Ref CI using larger basis sets. References are selected at only $r = 2.6\ a_0$. A threshold of 0.05 results in poor agreement with the CAS-Ref calculation, especially for the velocity TM, while the 0.025 threshold value agrees well with the CAS-Ref calculations. Thus we used the MRCI(0.025) treatment in our subsequent basis set study. As can be seen from Table 3, adding an additional *s*, *p*, and *d* ANO increases the length TM slightly, but yields a very small velocity TM; a reduction of a factor of 10 relative to the smaller [3*s* 2*p* 1*d*] basis set. Uncontracting the outermost *d* function reduces the velocity TM slightly, while uncontracting the outermost *s* and *p* primitives increases it slightly. However, the large difference between the length and velocity TMs is disconcerting considering the high level of treatment.

To assess the importance of the choice of the molecular orbital basis, we carried out a second basis set study using the orbitals from the 3-root SA-CASSCF based treatment—see Table 3. The reference list for the MRCI(0.025) treatment is that developed in the previous study [14] of C_2, and the reference selection is based on r values from 1.8 to 5.0 a_0. In the [3*s* 2*p* 1*d*] basis, the CAS-Ref treatment yields a length TM value that is in good agreement with the 2-root CAS-Ref results, but a poorer velocity TM. Adding 1*s* correlation reduces the velocity TM, but leaves the length value unaffected. The MRCI(0.025) and

MRCI CAS-Ref TMs agree well in the length representation, but the velocity TM is substantially smaller at the MRCI(0.025) level. In contrast to the 2-root SA-CASSCF calculation, uncontracting the outermost *d* function increases the velocity TM in the 3-root treatment. Note that we performed one calculation using the 3-root reference list with the 2-root orbitals and the velocity result was only slightly larger, suggesting that most of the difference is due to a change in the molecular orbital basis. Uncontracting the outermost *s* and *p* functions leads to a dramatic increase in the velocity TM. In this basis set, 1*s* correlation increases the velocity TM bringing it into reasonable agreement with the length value. Adding an *f* function reduces the velocity TM somewhat, while adding even-tempered diffuse functions increases the velocity TM slightly.

The final series of calculations used the [5*s* 4*p* 3*d* 2*f* 1*g*] ANO set with the outermost *s* and *p* or *s*, *p*, and *d* functions uncontracted and diffuse *s* and *p* functions added. In these very large basis sets the velocity TM was 87% of the length value. It is difficult to determine the origin of the remaining errors. For example, in the smallest basis sets, 1*s* correlation reduced the velocity TM while it increased the TM in larger basis sets. Furthermore, in the smallest basis set the MRCI(0.025) treatment yielded a transition moment in the velocity representation that was smaller than the CAS-Ref value. Thus the inclusion of more reference configurations might also increase the velocity TM.

The reason for the greater sensitivity of the velocity TM to the level of treatment becomes apparent from a consideration of Table 4, where we have decomposed the velocity and length TMs into their orbital contributions. The $[(4+1)s(3+1)p(2+1)d]$ MRCI(0.025) treatment with and without 1*s* correlation was used in this study. (Note that the $(n+m)$ notation gives the number of ANOs and uncontracted functions, respectively.) For the length TM, contributions greater than 0.01 au are included, whereas for the velocity TM only contributions greater than 0.1 au are included for brevity, since the velocity TM derives from a cancellation of many large contributions. Contributions are given both with and without 1*s* correlation included. There are no contributions from configurations involving holes in the 1*s* orbital that exceed these threshold values, although there are contributions that change the velocity TM by several hundredths of an au. The $X^1\Sigma_g^+$ and $A^1\Pi_u$ states differ nominally by the $3\sigma_g-1\pi_u$ single excitation, so that the $3\sigma_g-1\pi_u$ density matrix element is by far the largest. Although this matrix element makes the largest contribution to the length TM, this is not the case in the velocity representation due to the relatively small velocity integral corresponding to this matrix element. In fact, the largest contribution, which comes from the $1\pi_g-2\sigma_u$ matrix element, is over four times larger. Large contributions even arise from high-lying virtual orbitals with relatively small density matrix elements, because of the very large velocity integrals. Note that the velocity integrals in Table 4 have not been divided by the energy difference (0.024 au), whereas the velocity contributions have been. Clearly the sensitivity of the velocity TM to the level of treatment is related to the fact that significant contributions arise from many parts of the wave function. This effect may be exaggerated in this case by the multiconfigurational character of the ${}^1\Sigma_g^+$ state, but the general observations are expected to hold for most systems.

It is also of interest to determine how the agreement between the length and velocity TMs changes with *r*. In Fig. 1 we show the *r* dependence of the $A^1\Pi_u-X^1\Sigma_g^+$ TM in the length and velocity representations using the $[(4+1)s(3+1)p(2+1)d]$ MRCI(0.025) treatment without 1*s* correlation included. Although the velocity and length TMs agree relatively well at small *r*

Table 4. Individual contributions (au), density matrix elements, and integrals in the length and velocity representations of the total moment[a]

Transition element ${}^1\Sigma_g^+-{}^1\Pi_u$	Contribution[b]		Density element		Integral
	with 1*s*	no 1*s*	with 1*s*	no 1*s*	
		Length representation			
$2\sigma_g-1\pi_u$	0.01016	0.01033	−0.01245	−0.01266	−0.81617
$3\sigma_g-1\pi_u$	−0.05138	−0.05209	−0.12766	−0.12943	0.40245
$1\pi_u-3\sigma_g$	0.48357	0.48360	1.20158	1.20166	0.40245
$1\pi_u-4\sigma_g$	0.01932	0.02026	−0.03173	−0.03328	−0.60888
$2\sigma_u-1\pi_g$	−0.04041	−0.04043	−0.05017	−0.05021	0.80537
$1\pi_g-2\sigma_u$	−0.06161	−0.06047	−0.07650	−0.07509	0.80537
$1\pi_g-3\sigma_u$	−0.01027	−0.01031	−0.03508	−0.03522	0.29272
		Velocity representation			
$2\sigma_g-1\pi_u$	0.18448	0.19053	−0.01245	−0.01266	0.36279
$14\sigma_g-1\pi_u$	0.14715	0.15241	−0.00734	−0.00748	0.49079
$1\pi_u-2\sigma_g$	0.12915	0.16035	0.00872	0.01065	−0.36279
$1\pi_u-3\sigma_g$	−0.16511	−0.16778	1.20158	1.20166	0.00337
$1\pi_u-4\sigma_g$	0.27908	0.29739	−0.03173	−0.03328	0.21538
$1\pi_u-5\sigma_g$	−0.12761	−0.13676	−0.03459	−0.03649	−0.09034
$1\pi_u-6\sigma_g$	0.15271	0.15819	−0.01300	−0.01326	0.28758
$1\pi_u-14\sigma_g$	−0.11169	−0.11491	−0.00557	−0.00564	−0.49079
$4\pi_u-3\sigma_g$	−0.26521	−0.27978	0.01260	0.01308	0.51562
$5\pi_u-3\sigma_g$	−0.11539	−0.11441	−0.01553	−0.01515	−0.18199
$1\pi_u-2\delta_g$	−0.10322	−0.10615	−0.00515	−0.00521	−0.49079
$2\delta_g-1\pi_u$	0.14549	0.15050	−0.00726	−0.00739	0.49079
$2\sigma_u-1\pi_g$	−0.48691	−0.49508	−0.05017	−0.05021	−0.23766
$1\pi_g-2\sigma_u$	0.74245	0.74044	−0.07650	−0.07509	0.23766
$4\pi_g-2\sigma_u$	0.21793	0.22249	−0.01519	−0.01526	0.35130
$6\pi_g-2\sigma_u$	0.10008	0.10132	0.00518	0.00516	−0.47305

[a] The calculations were carried out at the MRCI(0.025) level of correlation treatment using the $[(4+1)s(3+1)p(2+1)d]$ basis set at $r = 2.6\,a_0$

[b] The factor of ΔE^{-1} has been included in the velocity contribution, but not in the integrals

values, they diverge as the avoided crossing is approached. However, it should be noted that the behavior of the velocity TM may be partially dictated by the fact that the $X^1\Sigma_g^+$ and $A^1\Pi_u$ states also cross in this region, so that the sensitivity of the velocity TM may be enhanced by the very small energy separation. Thus, although this band system may represent a particularly severe test case for the velocity TM, the velocity representation is incapable of providing even qualitatively correct results here.

4. Conclusions

We have studied four Rydberg transitions in H_2, the $A^1\Pi-X^1\Sigma^+$ transition in BH, and the $A^1\Pi_u-X^1\Sigma_g^+$ band system in C_2 in both the length and velocity representations. For all six transitions the velocity representation converges much more slowly, as both the one- and *n*-particle requirements are much more severe. The velocity TM is also far more sensitive to the effects of core correlation.

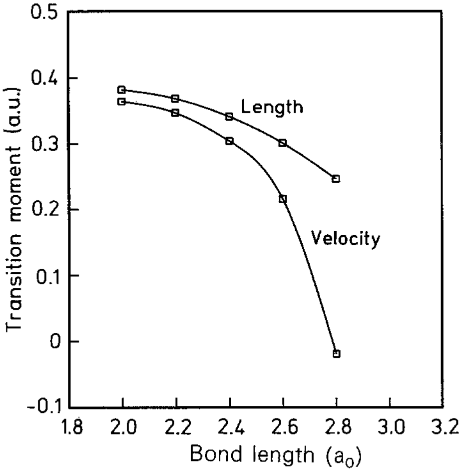

Fig. 1. The C_2 $A^1\Pi_u$–$X^1\Sigma_g^+$ transition moment as a function of r in the length and velocity representations

Thus for the bound-bound molecular transitions considered here, the velocity TM does not even constitute a viable diagnostic for the convergence of the length TM. For the transitions in H_2 the velocity and length TMs agreed reasonably well even when the moment had not converged with respect to the one-particle basis. In BH the velocity TM converged more slowly with basis set improvement and required core correlation to bring it into agreement with the length TM. For the $A^1\Pi_u$–$X^1\Sigma_g^+$ transition in C_2, the velocity TM is so sensitive to the level of treatment that it is difficult to demonstrate any degree of convergence. Thus this work argues strongly against the use of the velocity gauge as a judge of the reliability of conventional one-particle/n-particle space-type wave functions.

Acknowledgements. The authors would like to thank Ken Dyall, Knut Faegri, Harry Partridge, and Peter Taylor for helpful discussions.

References

1. Bauschlicher CW, Langhoff SR, Taylor PR (1990) Adv Chem Phys 77:103
2. Bethe HA, Salpeter EA (1957) Quantum Mechanics of One- and Two-electron Atoms. Springer, Berlin Heidelberg New York
3. Schiff B, Pekeris CL, (1964) Phys Rev A 3:638
4. Martin RL, McMurchie LE, Davidsion ER (1978) Int J Quantum Chem 13:161
5. Pindzola MS, Kelly HP (1975) Phys Rev A 12:1419
6. Almlöf J, Taylor PR (1987) J Chem Phys 86:4070
7. Bauschlicher CW, Taylor PR (1988) Theor Chim Acta 74:63
8. MOLECULE-SWEDEN is an electronic structure program system written by J Almlöf, CW Bauschlicher, MRA Blomberg, DP Chong, A Heiberg, SR Langhoff, P-Å Malmqvist, AP Rendell, BO Roos, PEM Siegbahn and PR Taylor
9. Huber KP, Herzberg G (1979) Constants of Diatomic Molecules. Van Nostrand Reinhold, New York
10. Rothenberg S, Davidson ER (1967) J Mol Spectrosc 22:1
11. Duijneveldt FB van (1971) IBM Research Report No. RJ 945
12. Bauschlicher CW, Langhoff SR, Taylor PR (1990) J Chem Phys 93:502
13. ONeil SV, Rosmus P, Werner H-J (1987) J Chem Phys 87:2847
14. Langhoff SR, Bauschlicher CW, Rendell AP, Komornicki A (1990) J Chem Phys 92:6599